This article has been accepted for publication in a future proceedings of this conference, but has not been fully edited. Content may change prior to final publication. Citation information: DOI: 10.1109/UPEC57427.2023.10294567, 2023 58th International Universities Power Engineering Conference (UPEC)

Wireless Power Transfer System for Electric Vehicle Charging with Frequency Hopping – A Concept and Circuit Design.

Graham Blankson
Department of Electronic and Electrical Engineering
Brunel Universisty London
London, United Kingdom
Graham.Blankson@brunel.ac.uk

Mohamed Darwish
Department of Electronic and Electrical Engineering Brunel Universisty London
London, United Kingdom
Mohamed.Darwish@brunel.ac.uk

Chun Sing Lai
Department of Electronic and Electrical Engineering
Brunel Universisty London
London, United Kingdom
Chunsing.Lai@brunel.ac.uk

***Abstract*—With the apparent reliability of wireless power transfer technology, Original Equipment Manufacturers are gradually migrating electric vehicle production charging modes from conductive to wireless. The increased users of electric vehicle wireless power transfer will introduce additional electromagnetic signals in the low frequency bandwidth which could cause interferences to various wireless operating systems. It is worth noting, vice versa, that the operation of the wireless power transfer can also be affected by near field propagated electromagnetic signals. This study shows a simplistic method to secure the electric vehicle's wireless power transfer operation from interference by providing simple resonant frequency hopping. A wireless power transfer system with a consolidated 85kHz, recommended by the Society of Automotive Engineers and non-standardized operating frequency of 250kHz was designed to this effect. The selection of 250kHz was based on a separate study detailed in this report.**

Keywords— ***Wireless Power Transfer, Frequency Hopping, Power Transfer Efficiency, Impedance Matching Circuit, Interoperability***

I. Introduction

As the popularity of the electric vehicle (EV) increases so does the need for the battery charging facilities. As at 2021 there were about 40.3 million licensed vehicles in the UK, most of which are internal combustion engine (ICE) vehicles and 8,365 petrol stations in the UK [1,2]. Based on the 2022 EV market statistics there are over 735,000 battery EVs and 480,000 plug-in hybrids in the UK [3] this number of EVs are bound to increase meaning that charging facilities are to be equally or more available in comparison to the ICE vehicles and petrol stations.

About 8.8kWh of energy is stored in a litre of petrol and a compact ICE vehicle can contain 60 liters of petrol which is about 500kWh, a similar size of EV will typically have 75kWh stored in its batteries [4]. The battery having a lower energy density than petrol will need more frequent recharges to achieve a comparable range to that of the conventional ICE vehicle. This shows the pressing need to extend the range of the EV safely thus the development of more sophisticated EV charge points. The dwell time for both conductive and wireless EV during charging appears as a mounting problem to the short range EV batteries cover on a full charge. The major way EV's are charged are by conductive charging where an electric cable is connected to the vehicle to charge its batteries. These chargers are vulnerable to vandalism and theft and obviously pose a potential hazard thus exposing the user to a degree of discomfort [6].

Wireless Power Transfer (WPT) is the technology of transferring electric energy wirelessly from a source to its load using resonant magnetic flux. WPT technology has been commonly used in electronic devices such as mobile phones, electric toothbrushes, inductive cookers, and biomedical equipment, and now being used for EV charging [5,7]. The Qi standard defines parameters for low power WPT (5W to 15W) at 100kHz operating frequency [8,9]. The demand curve for EV WPT becomes steeper every year due to the elegance, hands free, clean, futuristic, autonomous, speed, safe, cost effective and reliable aspects it provides the user [6]. In the UK the government announced the end of sales of new ICE cars by 2030 which leads the way to the manufacturing of new EVs and their essential electric chargers.

WPT technology provides a solution not only to charge the EV but to provide security, comfort and style to the customer during charging sessions. WPT provides an avenue for charging driverless EVs as it has the basic properties of being fully automated [6].

However, there is a risk that the electromagnetic (EM) propagation of the WPT could cause some level of interference on surrounding equipment and Internet of Things (IoT) and other wireless networks [10]. It is expedient to note that there is unrestricted placement of WPT units around the city and at times in car parks located at hospitals, industrial areas, railway stations etc, where interferences could occur. There are reports of WPT EM propagation interfering with amplitude modulated (AM) radio station signals [11]. There is further concern that the power supplied from the WPT is vulnerable to theft [12], and subject to frequency jamming. By implementing an alternative operating resonant frequency in the WPT circuit, the WPT can overcome these interferences and successfully complete its given charging session. Frequency hopping provides benefits including mitigating interferences, flexibility, reliability, coexistence with IoT and other signal equipment, security, and compliance with regulatory requirements at a global scale.

This article has been accepted for publication in a future proceedings of this conference, but has not been fully edited. Content may change prior to final publication. Citation information: DOI: 10.1109/UPEC57427.2023.10294567, 2023 58th International Universities Power Engineering Conference (UPEC)

This report discloses the concept and detail design of the circuit and considerations of the WPT EM emission and system power losses when operating at 250kHz. This report details research on possible power transfer efficiency (PTE) optimization by increasing the WPT operating frequency from 85kHz to 250kHz for a 10Ω load. The contribution of this work is broken down to four main parts:

1. Implemntation of frequency hopping.
2. Increment of operating frequency to enhance WPT interoperability in the frequency domain and determine the impact higher frequencies than 85kHz will have on the WPT efficiency.
3. Consolidation of a Low frequency and High frequency WPT system.
4. Identifying the coil configuration which can optimize power transfer efficiency (PTE) at both 85kHz and 250kHz, and also mitgate the EM emissions propagated during charging sessions.

II. CIRCUIT THEORY FOR WPT

The WPT technology is based on Faraday's law of induction and Amperes circuital law. On the transmitter unit or EV charger, Amperes circuital law is implemented. Amperes law states that the product of the magnetic field (or area of influence) and sum of the length element in the circuit is proportional to the product of the electric current passing through the circuit and the permeability of its circuit's conductor.

$$\int B_t * dl = \mu_0 * IN \quad (1)$$

Where B_t, dl, μ_0, I, N_p are varying magnetic flux with time, length of conductor, permeability of free space, current and number of turns in the winding respectively.

At the receiver unit or EV, Faraday's law of induction equation is executed. Faradays law determines the voltage generated in a wire within an alternating magnetic field.

$$E = N\frac{d\Phi}{dt} \quad (2)$$

Where *E, N* and $\frac{d\Phi}{dt}$ are back electromotive force or voltage, number of turns and rate of change of flux. The equivalent circuit of a WPT is shown in Fig. 1 where the transmitter circuit is on the left-hand side and the receiver circuit is on the right-hand side.

For a series - series WPT configuration as shown in Fig. 1 where the inductance of the transmitter coil and receiver coil are equal, we have

$$L = L_p = L_s \quad (3)$$

$$M = k\sqrt{L_p * L_s} \quad (4)$$

$$M = kL \quad (5)$$

Where *M, k, L, L_p and L_s* are mutual inductance, coupling coefficient, self-inductance, primary coil inductance and secondary side inductance.

To determine the operating frequency (OpF) the WPT circuit is modelled using voltage dependent sources as shown in Fig 2 where in the transmitter circuit's, V_p is voltage, i_p is current, R_p is the parasitic resistance, $1/(j\omega C_p)$ is the frequency dependent capacitive impedance, $j\,\omega\,L_p$ is the frequency dependent inductive impedance. Also in the receiver circuit, V_s is Voltage, i_s is current, R_s is the parasitic resistance, $1/(j\omega C_s)$ is the frequency dependent capacitive impedance, $j\omega L_s$ is the frequency dependent inductive impedance, R_L is the battery load resistance and ω is the angular operating frequency $2\pi f$.

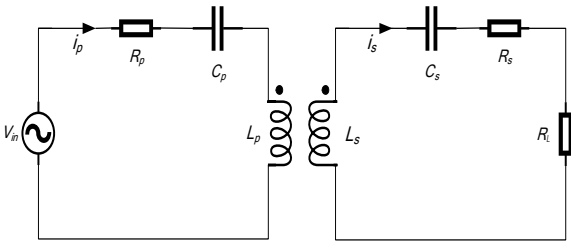

Fig. 1. Equivalent circuit of WPT showing the transmitter and receiver circuit.

Analyzing the receiver circuit

$$i_s = \frac{j\omega M i_p}{R_s+R_L+j\omega\left(L_s-\frac{1}{Cs}\right)} \quad (6)$$

Let $Z_s = R_s + R_L + j\left(\omega L_s - \frac{1}{\omega Cs}\right)$

$$i_s = \frac{j\omega M i_p}{Z_s} \quad (7)$$

Z_s is the total impedance in receiver side circuit. Hence, reflected impedance in transmitter side winding.

$$j\omega M i_s = \frac{\omega^2 M^2}{Z_s} i_p \quad (8)$$

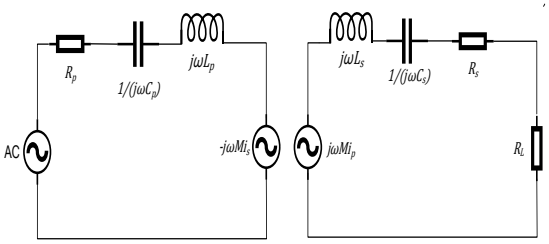

Fig. 2. WPT circuit showing dependent voltages.

Analyzing the transmitter circuit

$$i_p = \frac{V_{in}}{R_p+j\left(\omega L_s-\frac{1}{\omega C_s}\right)+\frac{\omega^2 M^2}{Z_s}} \quad (9)$$

Let $Z_p = R_p + j\left(\omega L_p - \frac{1}{\omega C_p}\right)$

Z_p is the total impedance in the transmitter circuit

$$i_p = \frac{V_{in}*Z_s}{Z_p Z_s+\omega^2 M^2} \quad (10)$$

$$i_s = \frac{j\omega M V_{in}}{Z_p Z_s+\omega^2 M^2} \quad (11)$$

At resonance $Z_p = R_p$ and $Z_s = R_s + R_L$ thus, Power in, P_{in} at resonance

$$P_{in} = \frac{{V_{in}}^2*(R_s+R_L)}{R_p R_s+R_p R_L+\omega^2 M^2} \quad (12)$$

Power out, P_{out}

$$P_{out} = \frac{\omega^2 M^2 {V_{in}}^2 * R_L}{\left(R_p R_s+R_p R_L+\omega^2 M^2\right)^2} \quad (13)$$

And efficiency, η

This article has been accepted for publication in a future proceedings of this conference, but has not been fully edited. Content may change prior to final publication. Citation information: DOI: 10.1109/UPEC57427.2023.10294567, 2023 58th International Universities Power Engineering Conference (UPEC)

$$\eta = \frac{P_{out}}{P_{in}} = \frac{\omega^2 M^2 * R_L}{(R_S+R_L)*(R_p R_S + R_p R_L + \omega^2 M^2)} \quad (14)$$

From this equation it is evident that the frequency ω, can have a possible effect on the efficiency, η.

III. Methodology and Selection of 250kHz

The society for Automotive Engineers' (SAE) recommended operating frequency for WPT is between 81.38kHz and 90kHz [13]. The non-standard 250kHz frequency was chosen based on results from assuming a 10Ω battery resistance which is about half of the load [14] used in their research. Modelling of the WPT was done on a finite element analysis software, Ansys Maxwell 3D, furthermore, the model was based on loading the WPT with 10Ω then increasing its operating frequency from 0Hz to 500kHz. A mathematical study was done to determine the linear relationship between efficiency and frequency for various battery internal resistance values as presented in Fig. 3. Both Ansys Maxwell 3D and mathematical results showed circa 30% PTE difference between 85kHz and 250kHz for the 10Ω battery resistance thus the reason of selecting 250kHz for the frequency hopping range.

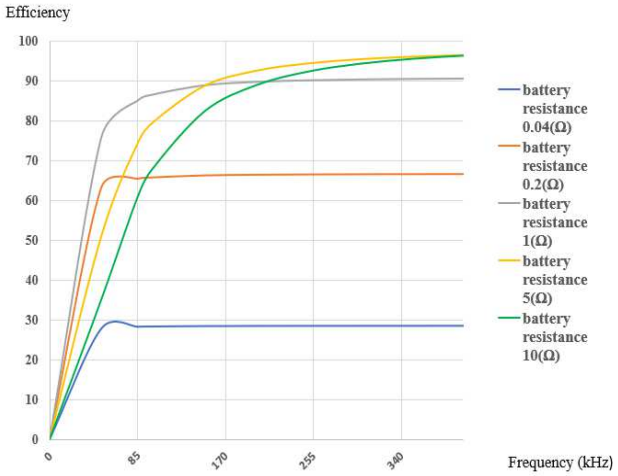

Fig. 3. Power Transfer efficiency of various EV battery internal resistances

A. Ansys model

The methodology of modelling and simulating the WPT's transmitter and receiver coils on Ansys is detailed in this section. A spiral coil having a self-inductance of 137.4uH with parameters of a 2mm diameter, 40 turns, 20mm inner diameter 0.1mm turn spacing, outer diameter of 188 mm and total length wire of 13.07m was modelled. For simplicity of the model a copper wire of 2mm diameter was used but, in the detailed design and construction, a 2mm diameter Litz wire with 16 individual strands whose diameter are not larger than .5mm shall be used. For the simulation the coil was excited with a current of 1A. This modelled coil of 137.4uH was duplicated to satisfy the transmitter and receiver coil modules. These coils were then separated by 180mm air gap.

In Ansys Simplorer, a simple WPT circuit was designed and powered with a 1V source voltage signal E1, at the resonant operating frequency (OpF) of 85kHz.

The coil modelled in Ansys Maxwell 3D was imported in Ansys Simplorer to simulate E1's OpFs between 0Hz and 500kHz, the capacitance values C1 and C2, were calculated on Ansys software using the equation.

$$C = \frac{1}{4*\pi^2*OpF^2*Ltx}. \quad (15)$$

The parasitic resistance, R1 and R2 is 0.1Ω, RLoad is 10Ω the self-inductances, L_{tx}, L_{rx} for the transmitter and receiver coils are 137.4uH. VM1, AM1, VM2, AM2 are the voltmeters and ammeters in the transmitter and receiver circuits as presented in Fig. 4. A frequency sweep from 0Hz to 500kHz was simulated to determine the PTE of various operating frequencies.

IV. Results

From the Ansys Simplorer frequency sweep Fig. 5. and Fig. 6. presents that at about 85kHz operating frequency the PTE is 44.3% and at 250kHz the PTE is 70.19%.

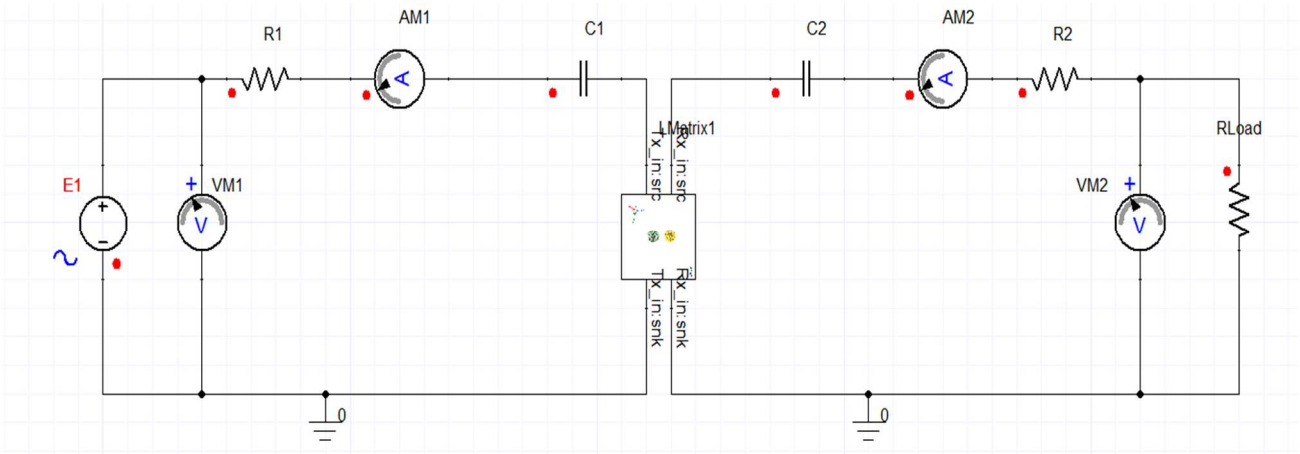

Fig. 4. Simulated 137.4uH 180mm air gap WPT circuit on Ansys – Simplorer

This article has been accepted for publication in a future proceedings of this conference, but has not been fully edited. Content may change prior to final publication. Citation information: DOI: 10.1109/UPEC57427.2023.10294567, 2023 58th International Universities Power Engineering Conference (UPEC)

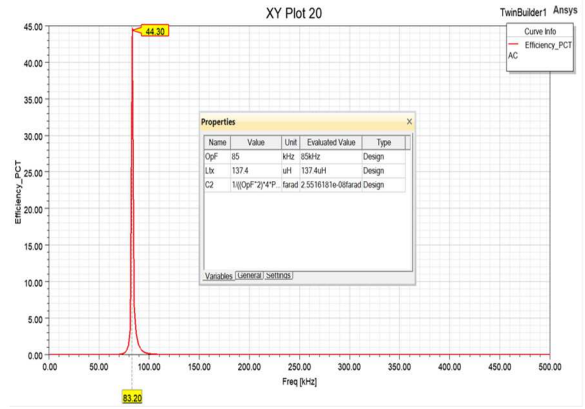

Fig. 5. PTE of 44.3% at 83.2kHz

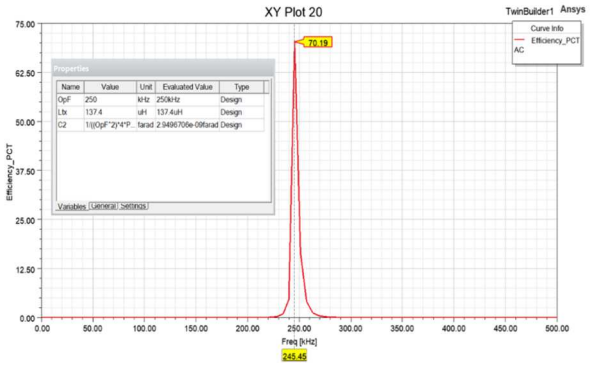

Fig. 6. PTE of 70.19% at 245.45kHz

V. Consolidation of a Low Frequency and High Frequency WPT

The major drive to consolidate the 85kHz and 250kHz WPT system is to provide frequency hopping. The new WPT EV charger is designed to charge at dual modes. As presented in Fig. 7, the rectifier in the transmitter unit is powered by 230V at 50Hz. The rectifier will convert the alternating current (AC) to direct current (DC). A tunable Signal Generator set to either 85kHz or 250kHz by the Frequency Selector Circuit (FSC) is connected to the gate drivers of the Inverter. This enables the inverter to operate at any of these frequencies.

At low frequency mode the FSC in Fig. 7, will convey a signal to the transmitter coil's variable capacitor control unit to set the variable capacitor C1, to resonate with the transmitter coil L1 at 85kHz OpF. The FSC will also transmit the signal to the self-resonating coil (SRC) L2's variable capacitor C2 to resonate at 85kHz. For the 250kHz mode, the same operation is completed to ensure the transmitter coil and SRCs operate at 250kHz OpF.

The SRCs form an essential part of the Impedance Matching Circuit (IMC). The SRCs are inductively coupled to the transmitter and receiver coils [5]. When an impedance mismatch due to misalignment occurs between the WPT's transmitter and receiver unit, the IMC shall detect and flag it to the user, giving the user the opportunity to either continue, stop its operation, or hop to the alternative OpF of the WPT see Fig. 7. The IMC in the receiver unit monitors the impedance of the receiver unit's coil and SRC and conveys that information to the transmitter unit's IMC to enhance the transmitter unit's IMC operation.

Power propagated from the transmitter coil induces a voltage at the receiver coil. As presented in Fig. 7, the high frequency AC induced voltage is converted to DC via the rectifier to charge the EV's battery, $R_{battery}$. It is assumed that the receiver circuit will default to a specific frequency initially. The receiver's IMC will continuously monitor the mutual inductance and coupling coefficient between the transmitter's SRC and transmitter coil and receiver's SRC and receiver coil and convey the data to the transmitter's IMC this is to ensure that the PTE is at its optimum level.

To initiate an EV charging session all operating status of the transmitter unit will be exchanged with the receiver unit via Zigbee Wi-Fi. During the charging session the receiver unit will transmit the OpF, battery state of charge and battery impedance provided by the EVs battery management system to the transmitter unit as presented in Fig. 7. Charging will

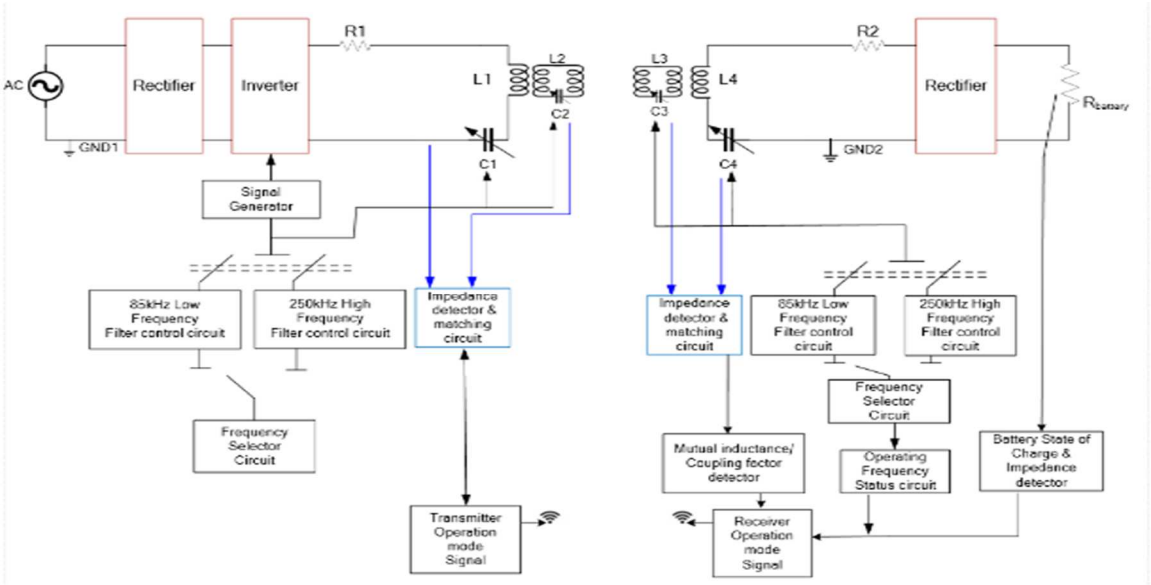

Fig. 7. Consolidated 85kHz and 250kHz WPT schematic

This article has been accepted for publication in a future proceedings of this conference, but has not been fully edited. Content may change prior to final publication. Citation information: DOI: 10.1109/UPEC57427.2023.10294567, 2023 58th International Universities Power Engineering Conference (UPEC)

commence once the transmitter unit's OpF mode is activated. If frequency interference is detected by the transmitter unit's IMC, the microcontroller will switch to the alternative OpF.

VI. Works Carried Out

To validate this proposal to increase WPT operating frequency to 250kHz a variety of factors have been determined. These include the efficiency of the DC-DC converter, power losses in the coils, coil configuration, EM emissions, and IMC that shall detect near field frequency interferences.

A. Coil design

As part of ongoing research to determine the difference in ohmic and eddy current losses at 85kHz and 250kHz initial studies were carried out on a 137.4uH spiral coil at 85kHz OpF.

The studies were carried out on Ansys Eddy Current Solver which showed a combined power loss of 12.55W at 85kHz for ohmic and eddy current. The equation

$$\delta = \frac{1}{\sqrt{\pi f \mu_0 \mu_r}} \qquad (16)$$

shows that the frequency, f when increased causes the skin depth, δ to reduce. Where δ, μ_0, μ_r are the skin depth, permeability of free space and relative permeability of copper. Theoretic calculations show a 223µm skin depth at 85kHz and 130µm skin depth at 250kHz on the 137.4uH spiral coil designed on Ansys Maxwell 3D. The coil modeled in Ansys Maxwell 3D was a 2mm diameter, 3.14mm^2 cross sectional area solid copper wire. From theoretic calculations based on the coil parameters, the AC resistance, $r_{a.c}$ at 85kHz is 36mΩ and at 250kHz it is 43mΩ.

The self-inductance of a particular length of wire depends on the final geometry of how it is wound. Since the inception of WPT, transmitter and receiver coil designs have been developed to optimize maximum PTE for wider air gaps. This is achieved when the coils are wound in a particular pattern that optimizes the self-inductance, mutual inductance, and quality factor. The fundamental challenge with the design of the transmitter coil is to maximize the quality factor and the geometrical arrangement [15]. Most coils are configured in the Rectangular, Circular, Double D (DD), DD Quadrature (DDQ) and Bipolar structure [5,6], [17].

An interoperable WPT study was carried out using a transmitter quadrature coil structure to transfer power to separate Circular, DD, and DDQ receiver coil structure units. The study showed that the DDQ coil structure portrays the maximum compatibility even under the misalignment conditions [15] however, factors like minimizing EM emissions were not assessed in the study. A bipolar coil configuration [18] shall be used for this frequency hopping WPT system as majority of the EM emissions will be canceled out.

VII. 100W WPT Circuit Design

From the initial studies carried out it was determined that the Ohmic losses between 85kHz and 250kHz OpFs will not be significant. Other studies showed that the EM emissions at 250kHz fall below the limits stipulated in INCIRP 2020 Guidance [16] when the coils are shielded. A prototype for the 100W frequency hopping WPT system has been developed on Altium Designer software. The prototype shall be subjected to various tests including the EM compatibility test to ensure it complies with the INCIRP 2020 Guidance. Circuit element specifications of the major subsystems in the frequency hopping WPT prototype shall be discussed.

A. Transmitter and receiver's FSC and IMC

The SRC on both transmitter and receiver units have a self-inductance of 137.4uF. In the FSC, a non-latching double pole double throw (DPDT) relay shall connect the coils to either set of capacitor banks to produce an OpF of 85kHz or 250kHz as presented in Fig. 8. The DPDT relay shall be controlled by a microcontroller.

The nodes "I N" and "I P" provide the voltage reference and the node "out1" provides the current reference for the IMC circuit see Fig. 8. These nodes are connected to the SRC and its associated capacitor bank in the FSC. The mutual inductance between the transmitter unit's SRC and the transmitter coil and the receiver unit's SRC and receiver coils, derived by the ratio of the voltage an current from these nodes are used to set and determine optimum PTE. The transmitter unit's IMC processes the data polled from the FSC's voltage and current nodes.

B. Transmitter's Rectifier and buck converter

A full bridge rectifier shall rectify the 230V 50Hz AC mains voltage to circa 325VDC. The 325VDC shall be stepped down to 12VDC via a GaN FET buck converter driven by a gate driver. The gate driver is pulsed at either 85kHz or 250kHz from the microcontroller. Also note that the

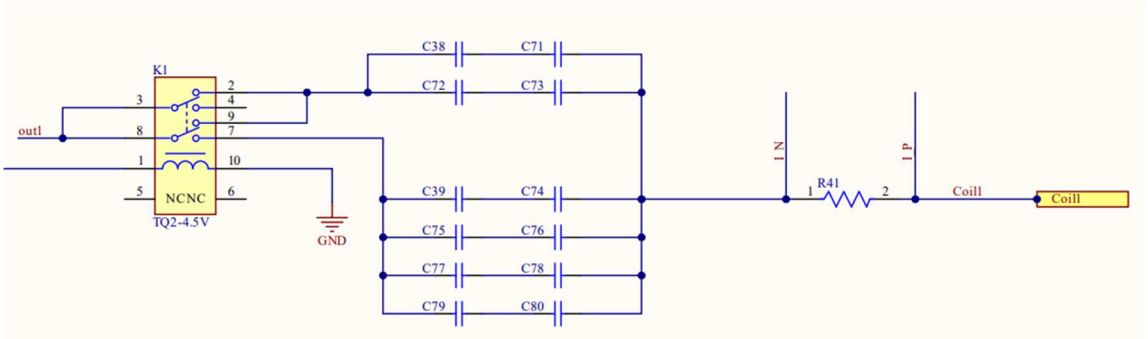

Fig. 8. Transmitter / Receiver side self-resonating coil subcircuit

microcontroller shall manage the IMC, FSC for frequency hopping, Wi-Fi and the user interface circuits.

C. Transmitter's Inverter

The 12VDC supply shall be delivered to the full bridge inverter circuit configured by four GaN FETs, and controlled by two gate drivers. The gate drivers shall be pulsed by the microcontroller at either 85kHz or 250kHz. It is anticipated that circa 12VAC and 4A shall be delivered to the transmitter coil from the inverter.

D. Receiver

The receiver circuit's configuration mirrors the transmitter. The high frequency AC voltage induced by the receiver coil shall deliver power to the full bridge rectifier mainly configured with 4 Schottky diodes. Power output from the rectifier shall be delivered to the buck converter configured with two GaN FETs and controlled by gate drivers. The receiver coil shall be connected to two banks of capacitors via a DPDT relay in order to operate at both 85kHz and 250kHz. The microcontroller, in the receiver circuit will manage the FSC, battery management system, IMC, Wi-Fi and communications. The SRC shall have the similar configuration as the transmitter circuit. The gate drivers shall be pulsed by the microcontroller at either 85kHz or 250kHz.

Table I. Parts list of major power module components

Device and designation	Part number
GaN FET for buck converter modules in both units	CRNLT125C65
Gate driver for buck converter module in both units and for Inverter module in transmitter unit	IR2101SPBF-BL
Microcontroller in both units	ESP32-S3-WROOM-1-N4R2
GaN FET for Inverter module in transmitter unit	EPC7003
Rectifier module in transmitter unit	GBU4J
DPDT relay for FSC module in both units	TQ2-4.5V
Schottky diode for full bridge rectifier module in receiver unit	MBR42050G

VIII. Conclusions and Future works

This paper presents the concept and detail design of the WPT with dual operating frequencies. It is a crude step to frequency hopping within the 85kHz and 250kHz bandwidth. It is envisaged that this WPT system shall provide the opportunity for operating at 85kHz and 250kHz, but studies and empirical formulae show that the frequency hopping shall not be limited to just two frequencies.

Future works on this design includes algorithm selection and programming of the microcontroller for the IMC subsystem, tendering of the bill of materials for procurement and PCB development. Additional works include simulations and measurements of Ohmic loss, GaN FET power losses, and verifications of EM force and EM compatibility of the WPT when operating at 250kHz. There is an aspiration that if the EM radiation test results at 250kHz operation mode comply with the ICNIRP guidelines it shall be shared with an original equipment manufacturer (OEM) as a valid proof of concept. Hopefully the EV and EV WPT charger's OEM shall consider implementing the frequency hopping technology in their existing 85kHz WPT systems.

IX. Refrences

[1] Driver & Vehicle Licensing Agency, "Vehicle licensing statistics: 2021," *GOV.UK*, May 24, 2022. Accessed: Jul. 19, 2023. [Online]. Available: https://www.gov.uk/government/statistics/vehicle-licensing-statistics-2021/vehicle-licensing-statistics-2021

[2] J. Aizarani. "Number of open petrol station sites in the United Kingdom (UK) from 2000 to 2022." Statista.com. https://www.statista.com/statistics/312331/number-of-petrol-stations-in-the-united-kingdom-uk (accessed Jul. 19, 2023).

[3] J. Edwards. "EV market stats 2023." Zap Map. https://www.zap-map.com/ev-stats/ev-market (accessed Jul. 19, 2023).

[4] O. N. Nezamuddin, C. L. Nicholas and E. C. d. Santos, "The problem of electric vehicle charging: state-of-the-art and an innovative solution," in *IEEE Trans. on Intell. Transp. Syst*, vol. 23, no. 5, pp. 4663-4673, May 2022, doi: 10.1109/TITS.2020.3048728.

[5] A. Triviño-Cabrera, J.M. González-González, J.A. Aguado "Fundamentals of wireless power transfer," in: *Wireless power transfer for Electric Vehicles: foundations and design approach*. Switzerland: Springer, 2020, 1-18.

[6] A. Mahesh, B. Chokkalingam and L. Mihet-Popa, "Inductive wireless power transfer charging for Electric Vehicles–a review," in *IEEE Access*, vol. 9, pp. 137667-137713, 2021, doi: 10.1109/ACCESS.2021.3116678

[7] W. M. G. Dyab, M. S. Ibrahim, A. A. Sakr and K. Wu, "Ridge gap waveguide enabled wireless power transfer for Electric Vehicle applications," *2020 50th Eur. Microw, Conf. (EuMC)*, 2021, pp. 852-855, doi: 10.23919/EuMC48046.2021.9338138.

[8] A. D. de Sousa, L. F. M. Vieira and M. A. M. Vieira, "Optimal transmission range and charging time for Qi-compliant systems," in *IEEE Trans. on Power Electron.*, vol. 35, no. 12, pp. 12765-12772, Dec. 2020, doi: 10.1109/TPEL.2020.2996999.

[9] Wireless power consortium "Qi." Wireless power consortium. Accessed: Jul. 19, 2023 [Online]. Available: https://www.wirelesspowerconsortium.com/qi

[10] J. Eidaks et al., "Experimental study on multi-hop wireless power transfer," *2023 IEEE 10th Jubilee Workshop on Advances in Inf., Electron. and Elect. Eng. (AIEEE)*, Vilnius, Lithuania, 2023, pp. 1-4, doi: 10.1109/AIEEE58915.2023.10134920.

[11] Randy J. Stine "Wireless EV Charging Could Pose Threat to AM Reception." RADIOWORLD. https://www.radioworld.com/tech-and-gear/wireless-ev-charging-could-pose-threat-to-am-reception(accessed Jul.23 2023).

[12] Y. Li et al., "A novel method of wireless power transfer identification and resonance decoupling based on frequency hopping communication," in *IEEE Access*, vol. 7, pp. 161201-161210, 2019, doi: 10.1109/ACCESS.2019.2950084.

[13] *Wireless Power Transfer for Light-Duty Plugin/Electric Vehicles and Alignment Methodology,* SAE J2954 Nov. 2018.RP, Society of Automotive Engineers, July 2023. [Online]. Available: https://www.sae.org/standards/content/j2954_202010

[14] A. Huang et al., "Optimal matching reactance design and validation in wireless power transfer system for Electric Vehicle based on SAE J2954-RP," in *2020 IEEE Wireless Power Transfer Conf. (WPTC),* 2020, pp. 174-177, doi: 10.1109/WPTC48563.2020.9295576.

[15] A. Ahmad, M. S. Alam and A. A. S. Mohamed, "Design and interoperability analysis of quadruple pad structure for Electric Vehicle wireless charging application," in *IEEE Trans. on Transp. Electrific*., vol. 5, no. 4, pp. 934-945, Dec. 2019, doi: 10.1109/TTE.2019.2929443.

[16] "Guidelines for limiting exposure to electromagnetic fields (100 kHz to 300 GHz)" *Health Physics* 118(5): p 483-524, May 2020. DOI: 10.1097/HP.0000000000001210.

[17] Y. Zhang, S. Chen, X. Li and Y. Tang, "Design of high-power static wireless power transfer via magnetic induction: an overview," in *CPSS Trans. on Power Electron. and Appl*., vol. 6, no. 4, pp. 281-297, Dec. 2021, doi: 10.24295/CPSSTPEA.2021.00027.

[18] T. Shijo et al., "85 kHz band 44 kW wireless power transfer system for rapid contactless charging of electric bus," *2016 Int. Symp. on Antennas and Propag. (ISAP),* Okinawa, Japan, 2016, pp. 38-39.